

## Participation of Halobacteria in Crystal Formation and the Crystallization Rate of NaCl

ALEJANDRO LOPEZ-CORTES  
JOSE-LUIS OCHOA  
RAFAEL VAZQUEZ-DUHALT

Division of Experimental Biology  
Center for Biological Research (CIB)  
Baja California Sur, Mexico

*The presence of extremely halophilic archaeobacteria in NaCl solution increased the number and size of cubic crystals of halite formed and also yielded dendritic crystals. Various dissolved and suspended materials such as glucose, glycerol, casein hydrolysate, amino acids, ferrocyanide, silica gel, eubacteria, halobacteria, and surface layers (S-layers) of Haloarcula strain SP8807 were evaluated for their ability to modify the crystal habit of halite. The results showed that whole cells and surface layers (S-layers) of Haloarcula strain SP8807 were able to induce the formation of dendritic crystals. Negative staining and sodium dodecyl sulfate polyacrylamide gel (SDS-PAGE) analysis suggest that the proteinaceous constituents of extremely halophilic archaeobacterial S-layers may determine the crystal form of halite.*

**Keywords** crystal habit, crystallization rate, halobacteria, sodium chloride, surface layers (S-layers)

The participation of microorganisms in the physicochemical development of brine has been recognized in recent years (Davis, 1978; Schneider & Herrmann, 1980; Jones et al., 1981; Javor, 1989). Ironically, the role that dissolved organic carbon plays in calcium carbonate and gypsum precipitation is much better known than its role in the formation of more economically important halite and potash minerals (Javor, 1989).

In salterns, the crystallizer ponds often appear red because of the presence of aerobic halobacteria. These microorganisms cause the ponds to heat faster and attain higher temperatures, thus accelerating their evaporation rate (Jones et al., 1981; Javor, 1989). It has been observed, however, that square halobacteria may actually hinder evaporation by inducing the formation of a salt crust on the brine surface (Krumbein, 1985). In addition, the crystals that form in solutions heavily loaded with halobacterial cells generally contain many more and larger fluid inclusions than crystals formed in sterile salt solutions (Norton & Grant, 1988).

Received 17 August 1993; accepted 31 May 1994.

This research is part of the doctoral thesis of A. Lopez-Cortes at the CCH-UNAM Biotechnology Program. The authors thank Dr. Sergio Sánchez-Esquivel and Dr. Amelia Farres for their encouragement and support during these studies; Dr. Susanne Schultze-Lam for valuable suggestions and comments; Dr. Eugenia Klein from the Weizmann Institute of Science for electron microscopy facilities; Ariel Cruz Villacorta for technical assistance; and Roy Bowers for English corrections.

Address correspondence to Dr. Alejandro Lopez-Cortes, Division of Experimental Biology, Center for Biological Research (CIB), Baja California Sur, P.O. Box 128, La Paz, B.C.S., 23000 Mexico.

The halobacterial genera are represented by neutrophilic or alkalophilic, gram-positive or gram-negative rods, cocci, and irregular plates (Grant & Ross, 1986). The gram-negative cells of the prokaryotic genera *Halobacterium*, *Haloarcula*, *Haloferax*, and *Natronobacterium* are surrounded outside the plasma membrane by surface layers (S-layers) as the exclusive cell-wall component (Messner & Sleytr, 1992). The most detailed structural and biosynthetic studies were done on the S-layer glycoprotein from *Halobacterium halobium* and *H. salinarum* (Sumper, 1987; Lechner & Wieland, 1989). Recently, Sumper et al. (1990) reported a partial chemical characterization of the S-layer glycoprotein of *Haloferax volcanii*.

There is a lack of experimental data on the influence of halobacterial S-layers on the modification of crystal habit and mineralization of halite crystals. It is known that organic and inorganic substances can modify the crystal shape of halite from cubic to other forms. For example, dendritic crystals were formed when NaCl solutions were mixed with ferrocyanide (Ploss, 1964; Shuman, 1965), but this compound is not found in natural evaporite environments (Javor, 1989). Here, we studied (1) the participation of halobacterial cells as seeds in the nucleation of halite and (2) the crystal formation of the halite as affected by the dissolved and suspended materials, glucose, glycerol, casein hydrolysate, amino acids, ferrocyanide, silica gel, halobacterial cells, and S-layers of extreme halophilic archaeobacteria, to increase the understanding of the relationships between halobacterial cells and crystalline halite.

## Materials and Methods

### *Strains and Growth Conditions*

The bacterial strains used were *Halobacterium halobium* NRC 817, *Haloarcula vallismortis* ATCC 29252, *Haloferax mediterranei* ATCC 33500, *Haloarcula* SP8807, *Vibrio parahaemolyticus* MMF6, *Planococcus* sp. M6P2, and *Azospirillum brasilense* Cd DSM 1843. The eubacteria *V. parahaemolyticus* and *Planococcus* were isolated from a hypersaline ecosystem (Guerrero Negro, B.C.S., Mexico), and *A. brasilense* is unrelated to hypersaline environment. These widespread eubacteria strains were included in this study to determine if they affect salt crystal formation. The halophilic bacteria were cultivated in HEC medium formulated in 25% seawater as follows (g/L): NaCl, 195; MgCl<sub>2</sub>·H<sub>2</sub>O, 16.25; MgSO<sub>4</sub>·7H<sub>2</sub>O, 25; CaCl<sub>2</sub>·2H<sub>2</sub>O, 0.6; KCl, 5; NaHCO<sub>3</sub>, 0.2; NaBr, 0.6; NH<sub>4</sub>Cl, 2.5; FeCl<sub>3</sub>·6H<sub>2</sub>O, 0.0062; KH<sub>2</sub>PO<sub>4</sub>, 0.62. The carbon and nitrogen sources were 5 g/L yeast extract and 1.0 g/L casein hydrolysate (Torreblanca et al., 1986). The cultures were incubated at 38°C and agitated at 150 rpm. *Azospirillum brasilense* was cultivated in nutrient broth (Merck, Germany) and incubated at 30°C under agitation.

### *Evaluation of Crystallization Rates*

Cultures in the exponential phase (200 ml) were centrifuged for 10 min, 16,000g at 4°C. The pellet was resuspended in 20 ml filter-sterilized 30% NaCl solution to OD<sub>540 nm</sub> of 1.5. Samples of the cell suspension were adjusted to densities between 10<sup>6</sup> to 10<sup>7</sup> cells/ml, comparable to those reported from natural evaporitic habitats (Norton & Grant, 1988), transferred to a plastic dish (8.5 cm diameter), and placed in an environmental chamber at 30 ± 0.4°C, 55% relative humidity, and light intensity of 170 μE m<sup>-2</sup> s<sup>-1</sup> without disturbance. The control consisted of 20 ml filter-sterilized 30% NaCl solution. The weight, number, and size (>1 mm) of formed crystals was determined every 4 h beginning at 15

h, after decanting the sodium chloride solution and drying at 60°C for 48 h. All experiments were carried out in triplicate.

#### ***Determination of the Number and Size of Halite Cubic Crystals with Scanning Electron Microscopy***

In order to assess whether halobacterial cells affect the number and size of crystals formed, it was necessary to look on a much smaller scale using scanning electron microscopy.

One milliliter of exponential-phase bacterial culture was centrifuged for 5 min, 16,000g at 20°C. The pellet was washed 3 times with filter-sterilized 30% NaCl solution and resuspended in the same solution. From this suspension, 5- $\mu$ l drops were placed on a glass coverslip that had been given a gold coating at 10 mA during 12 min, positioned on an aluminum pin-type mount previously coated with carbon-conductive, double-sided tape. The drops were incubated at a temperature of 24°C without disturbance. After 10, 20, and 30 min, excess brine was eliminated with filter paper. The specimens were air-dried and gold-coated at 20 mA during 8 min. The blank consisted of 5- $\mu$ l drops of sterile 30% NaCl solution treated under the same conditions. The specimens were viewed using a Philips 515 scanning electron microscope at an accelerating voltage of 25 kV.

#### ***Evaluation of Effect of Strains, S-Layers, and Chemical Materials on the Crystal Form of NaCl***

One milliliter of bacterial suspension from an exponential-phase culture was centrifuged for 5 min, 16,000g at 20°C. The pellet was washed 3 times with filter-sterilized 30% NaCl solution and resuspended in 1.0 ml of the same solution. From this suspension, 20 5- $\mu$ l drops were placed on a clean microscope slide and kept in a chamber for 24 h at 35°C and 40% relative humidity. The slides were observed with a phase-contrast microscope (Nikon Labophot, Japan) at low magnifications of 2.5 $\times$ , 10 $\times$ , and 20 $\times$ .

The following samples were mixed with filter-sterilized 30% NaCl solution: S-layers from strain SP8807 (20  $\mu$ g/ml); potassium ferrocyanide, glucose, glycerol, casein hydrolysate, and silica gel (63–200  $\mu$ m) from Sigma Chemicals Co., St. Louis, MO; and amino acids from Merck, Germany (8003–8004), at concentrations between 200 and 2000  $\mu$ g/ml. Twenty 5- $\mu$ l drops of each mixture were placed on clean microscope slides, dried, and observed as described earlier. The chemicals glucose, glycerol, and amino acids were chosen because they have been recognized as osmoregulators produced by halophilic microorganisms. The silica gel was chosen as an example of inert particles. The ferrocyanide was chosen for its ability to form dendritic crystals of halite previously reported by Ploss (1964) and Shuman (1965), and casein hydrolysate as an example of a peptide.

#### ***Preparation of S-Layers and Spheroplast of Haloarcula SP8807***

In order to know the bacterial structure involved in the modification of mineralization and the crystal habit of halite, we chose the S-layers because they are in continual contact with their environment. Recently it was proposed that the S-layer serves as a template for fine-grained gypsum and calcite formation (Schultze-Lam et al., 1992).

The surface layers were isolated as follows: One milliliter of culture in exponential phase was centrifuged for 5 min, 16,000g at 20°C. The pellet was resuspended in spher-

plasting solution composed of 0.1 M MES [2(*N*-morpholino)ethane sulfonic acid] buffer, pH 7.0, plus 0.5 M sucrose, 0.25 M NaCl, and 0.01 M MgCl<sub>2</sub> (Jarrell & Sprott, 1984). After 30 min of resuspension, the cells were converted into spherical bodies by a decrease in external sodium chloride and magnesium salt concentration. In this condition, the S-layers were removed and dissociated from the cell surface (Cohen et al., 1983; Hecht et al., 1986). The suspension was centrifuged for 5 min, 16,000g at 20°C, resulting in a spheroplast pellet and dissociated S-layer subunits in the supernatant.

The S-layer subunits were recovered and dialyzed (Sleytr et al., 1988) at 4°C against distilled deionized water with the solutes of the spheroplasting solution except sucrose. After dialysis, the S-layer subunits were reassembled in a salts solution composed of 4 M NaCl, 25 mM KCl, 80 mM MgSO<sub>4</sub>, pH 3.2 (Hecht et al., 1986). This procedure yielded spheroplasts and purified S-layers. The self-assembled S-layers were examined by SDS-PAGE and transmission electron microscopy and tested in mineral formation studies. For negative staining preparations, we also used a solution of 10 mM CaCl<sub>2</sub> at pH 6 to promote the reassembly of the S-layer subunits (Koval & Murray, 1986; Kessel et al., 1988).

### **SDS-PAGE**

Electrophoresis was done using PhastGels gradient 4–15% with PhastGel SDS buffer strips (Pharmacia, Sweden). The molecular mass markers were bovine albumin, 66 kDa; egg albumin, 45 kDa; glyceraldehyde-3-phosphate dehydrogenase, 36 kDa; bovine carbonic anhydrase, 29 kDa; bovine trypsinogen, 24 kDa; soybean trypsin inhibitor, 20.1 kDa; and  $\alpha$ -lactalbumin from bovine milk, 14.2 kDa (Sigma, SDS-7 Dalton Mark VII-L, USA). The gels were stained for protein by the silver impregnation method with PhastGel electrophoresis media (Pharmacia, Sweden) and periodic acid-Schiff (PAS) staining procedure for the detection of glycoproteins using the PhastSystem (Van-Seuningen & Davril, 1992).

### **Negative Staining for Electron Microscopy**

Negative staining preparations were done with fixed and unfixed self-assembled S-layers. Reassembled S-layers were prefixed in 3% (v/v) glutaraldehyde in buffer solution of 4 M NaCl, 25 mM KCl, 80 mM MgSO<sub>4</sub>, pH 3.2, for 1 h at 4°C in the dark. After this time the structures were centrifuged for 5 min, 10,000g at 20°C, and the supernatant was replaced by clean fixing solution under the same conditions. The fixed S-layers were washed and preserved at 4°C with the same buffer solution.

Drops (10  $\mu$ l) of fixed samples containing S-layer fragments were placed on a small sheet of Parafilm and diluted 1:40 with a buffer solution of 2 M NaCl, 12.5 mM KCl, 40 mM MgSO<sub>4</sub>, pH 3.2. Ten-microliter drops of sample were transferred immediately to copper grid previously exposed to glow discharge. After 3 min, each grid with sample was stained with 2–3 drops of 2% aqueous uranyl acetate for 1 min. Excess stain was removed by blotting with filter paper (Sleytr et al., 1988). Drops (10  $\mu$ l) of unfixed samples containing reassembled S-layer in solution of CaCl<sub>2</sub> (10 mM, pH 6) were also placed on copper grids previously exposed to glow discharge. After 3 min, each grid with sample was stained with 2–3 drops of 2% aqueous uranyl acetate for 1 min. Excess stain was removed by blotting with filter paper (Sleytr et al., 1988). All specimens were viewed in a Philips 410 transmission electron microscope at an accelerating voltage of 80 kV.

## Results and Discussion

### Crystallization Rates

We found no significant differences in the weight of sodium chloride crystals harvested with or without halobacteria (Figure 1); however, the halobacteria affected the number and size of the sodium chloride crystals (Figure 2). In Figure 2 we disregarded crystals smaller than 1 mm. We analyzed our data by a one-way analysis of variance (ANOVA) test to evaluate the effect of halobacterial cell morphology on crystallization rates. The number of crystals formed in the presence of the three bacterial strains differed significantly from the control (Figure 2). While the control produced few but homogeneously sized crystals, the presence of halobacteria produced many cubic crystals of different size, some of them large, 25 mm per side (Figure 2). The one-way analysis of variance showed two types of response to halobacteria: one to cells of *H. vallismortis* and *Haloarcula* strain SP8807 that have an angular shape, and the other to cells of *H. halobium*, which are rod-shaped (Grant & Ross, 1986). This difference in response could be explained by the cell shape: that is, bacteria with triangular or square shapes (*Haloarcula* spp.) provide a template that mimics the crystal structure and thus serves as a means of mechanical nucleation, similar to the way foreign particles act as seeds or nuclei to promote crystal formation in saturated solutions (Norton & Grant, 1988).

The formation of a greater number of cubic crystals in the presence of halophilic archaeobacteria was confirmed at the micrometer level (Table 1 and Figure 3).

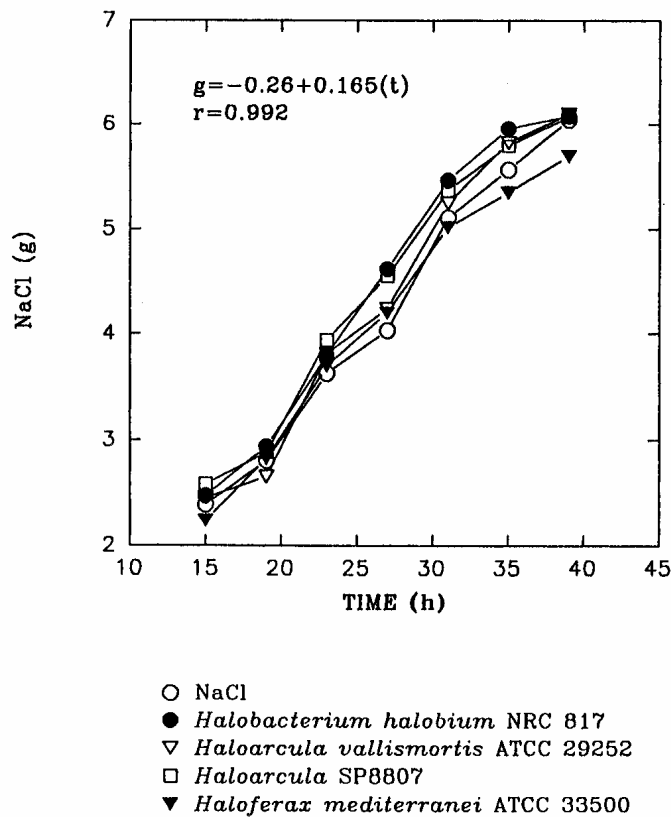
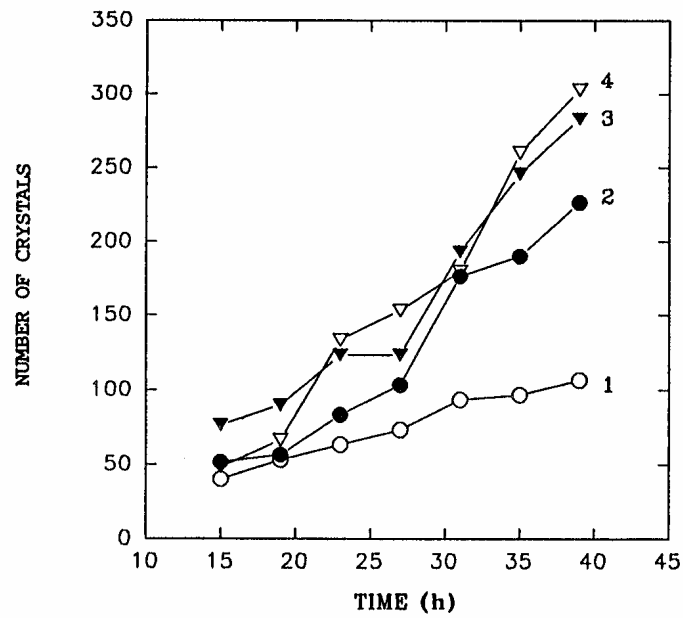


**Figure 1.** Effect of halobacteria on sodium chloride harvested from 30% NaCl solution (in grams). The equation corresponds to the control.



- 1 NaCl (1-8 mm)
- 2 *Halobacterium halobium* NRC 817 (1-25 mm)
- 3 *Haloarcula vallismortis* ATCC 29252 (1-15 mm)
- 4 *Haloarcula* SP8807 (1-15 mm)

**Figure 2.** Influence of halobacteria on the number and size of halite crystals. To facilitate our study, we only considered crystals larger than 1 mm. The data were analyzed by a one-way analysis of variance (ANOVA) test with a confidence of  $p \leq .05$ .

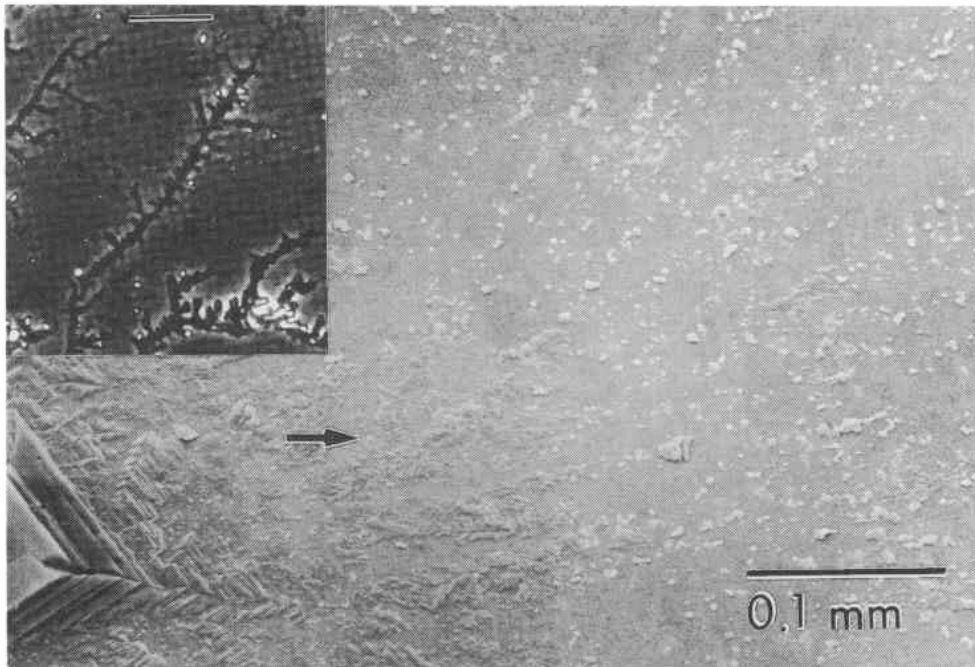


**Figure 3.** Overall crystal formation trends in the presence of *Haloarcula* strain SP8807 cells. The bar represents 0.1 mm. Note the great number of particles that make up the dendritic shape (arrow). The inset shows a photomicrograph of dendritic sodium chloride crystals produced by the addition of cells of *Haloarcula* strain SP8807. The bar represents 25  $\mu\text{m}$ .

### Crystal Formation of NaCl

Halite has a crystalline form based on cubic symmetry. Microscopy of evaporating drops of brine, however, has revealed crystal forms of sodium chloride other than cubes (Ploss, 1964; Shuman, 1965).

The presence of *Haloarcula* strain SP8807 caused the formation of dendritic crystals of halite (inset, Figure 3). The scanning electron microscopy (SEM) micrograph of Figure 3 shows overall crystal formation trends in which dendritic crystals are outside and between cubic crystals. Examination of dendritic crystals at high magnification showed a relationship between the halobacteria and the surface of halite crystals, and also confirmed that these cells modified the crystal habit, resulting in irregular shapes of halite (Figure 4). Other strains of halobacteria were also capable of inducing formation of dendritic crystals. Although the halophilic eubacteria *V. parahaemolyticus* and *Planococcus* that we tested were isolated from hypersaline environments, they did not produce dendritic crystals, which suggests that not all microbes present in crystallizer ponds are involved in the modification of crystal habit. The specific influence of halobacteria in the modification of crystal habit was also confirmed by the inability of *A. brasilense*, an organism that does not occur in hypersaline environments, to form dendritic crystals, which may be explained by the different chemical composition and structure of its cell surface.

SDS-PAGE analyses of purified S-layer of *Haloarcula* SP8807 showed a single band of protein with molecular mass of 66 kDa (Figure 5). However, the staining procedure for the detection of glycoproteins did not show bands.

It is well known that the S-layers of most halophilic archaeobacteria appear to be composed of glycoproteins (Messner & Sleytr, 1991). A report on the detailed chemical structure of glycopeptide of *H. salinarum* (Sumper, 1987) and the primary structure of the cell surface glycoprotein of *H. halobium* (Lechner & Sumper, 1987) has confirmed the original data (Mescher et al., 1974; Mescher & Strominger, 1976). The cell surface glycoprotein of *H. halobium* has a molecular mass of about 120 kDa (core protein = 87 kD). Recently, Sumper et al. (1990) reported a partial chemical characterization of the S-layer glycoprotein of *Haloferax volcanii* in which the mature polypeptide contains 794 amino acids with a calculated molecular mass of 81 kDa. Although glycosylation is not an

**Table 1**  
Effect of *Haloarcula* strain SP8807 on the number and size ranges of cubic crystals formed

| Size Ranges<br>( $\mu\text{m}$ ) | Number of Crystals from<br>30% Solution of NaCl<br>(Control) |               | Number of Crystals from<br><i>Haloarcula</i> , $1 \times 10^7$ cells/ml |                |
|----------------------------------|--|---------------|---|----------------|
|                                  | 30 $\times$  | 200 $\times$  | 30 $\times$   | 200 $\times$   |
| 1–100                            | 159 $\pm$ 75   | 432 $\pm$ 220 | 706 $\pm$ 23  | 1217 $\pm$ 421 |
| 101–200                          | 43 $\pm$ 4   | 12 $\pm$ 4    | 58 $\pm$ 29   | 13 $\pm$ 7     |
| 201–300                          | 12 $\pm$ 3   | 2 $\pm$ 1     | 12 $\pm$ 5  | 1 $\pm$ 1      |
| 301–400                          | 6 $\pm$ 1  | 0             | 5 $\pm$ 1   | 0              |

*Note.* The numbers of crystals listed are the sum of the counts at 30 $\times$  and 200 $\times$  magnification, respectively, from 10-, 20-, and 30-min incubations, determined by scanning electron microscopy.

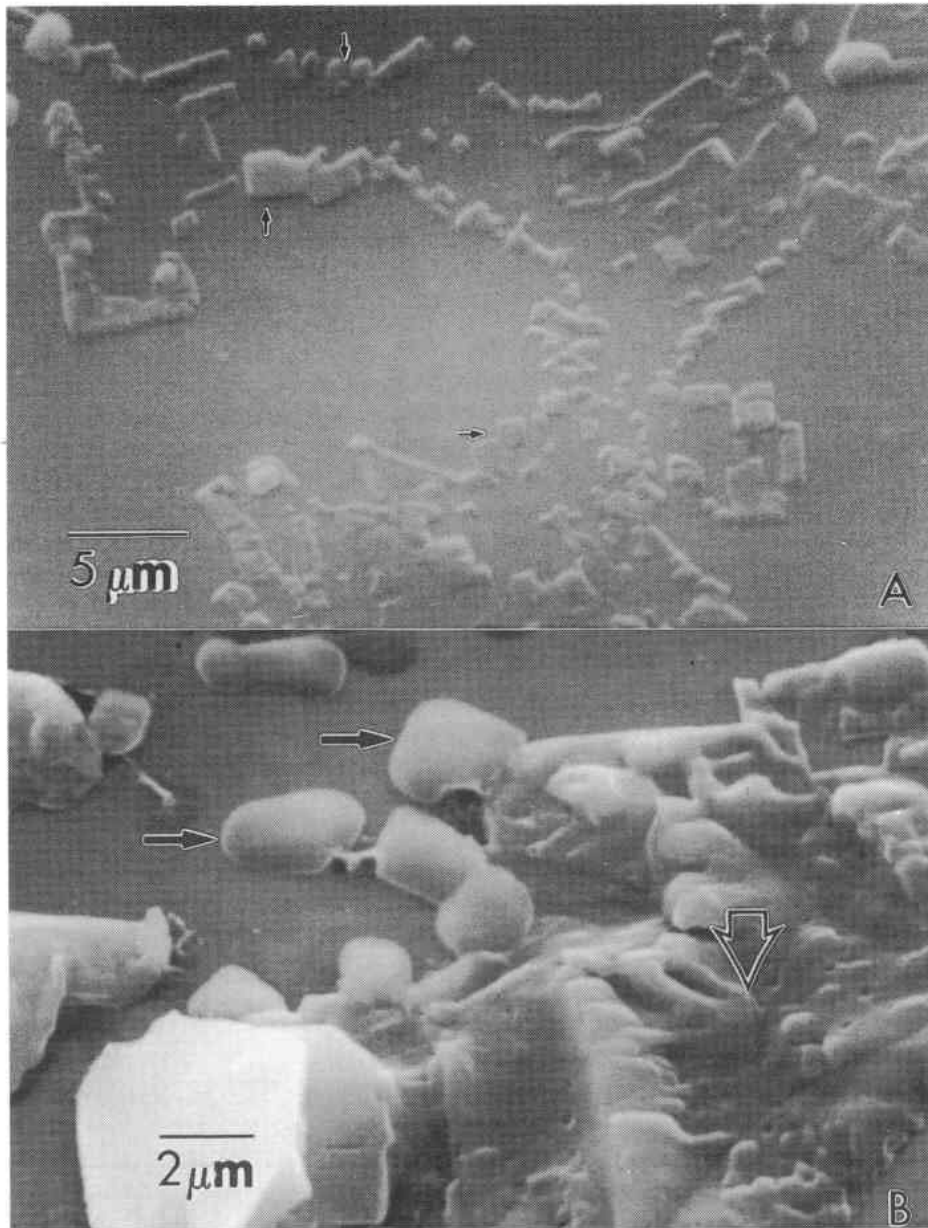


**Figure 4.** Details of the form of dendritic crystals. (A) The dendritic shape was built by flat cubic microcrystals (arrows). The bar represents 5  $\mu\text{m}$ . (B) High magnification also shows the presence of halobacterial cells (arrows) combined with amorphous halite crystals (empty arrow). The bar represents 2  $\mu\text{m}$ .

obligatory step in S-layer biosynthesis, it represents an important protein-modification reaction that can add great potential for the diversification of bacterial cell surface properties (Messner & Sleytr, 1992). In this context, it is interesting to note that upon continuous cultivation under optimal conditions, some bacterial strains have lost their ability to glycosylate S-layer proteins (Messner & Sleytr, 1991).

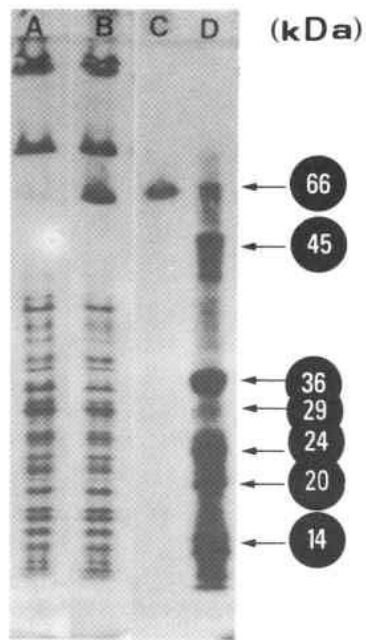


**Figure 5.** SDS-PAGE 4–15% gradient gel, silver stain. Lanes: A, profile of proteins from spheroplasts of *Haloarcula* SP8807; B, profile of whole-cell protein from *Haloarcula* SP8807; C, purified S-layer subunits from *Haloarcula* SP8807; D, profile of molecular-weight markers.

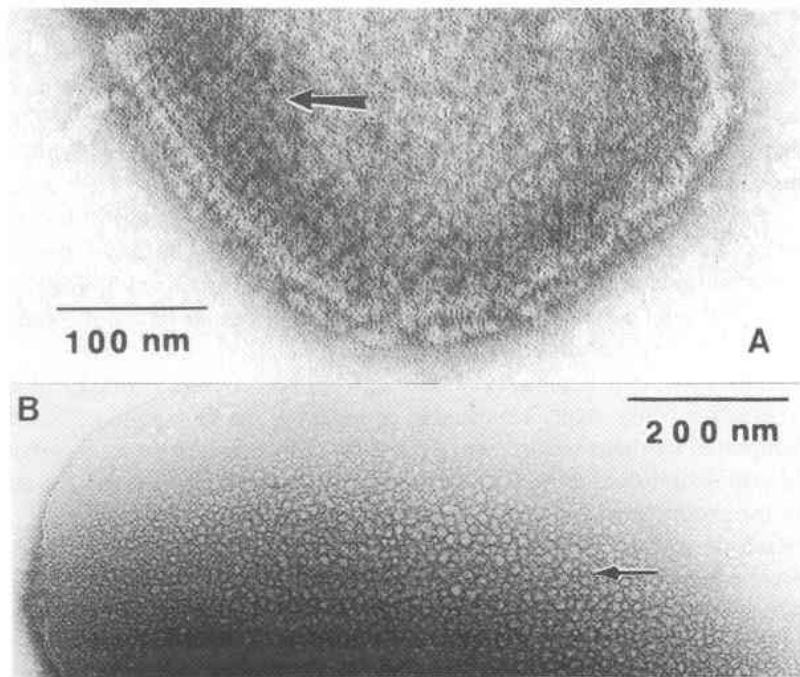


**Figure 6.** Negatively stained (2% uranyl acetate) preparations of S-layer self-assembly products of *Haloarcula* SP8807. (A) Unfixed S-layer reassembled in 10 mM  $\text{CaCl}_2$  at pH 6. The arrow shows an area with a hint of periodicity in one dimension. (B) Flat sheet-line S-layer self-assembled, which shows a honey comb appearance of a hexagonal arrangement of the morphological units (arrow). Stained in the presence of a solution composed of 2 M NaCl, 12.5 mM KCl, 40 mM  $\text{MgSO}_4$  pH 3.2.

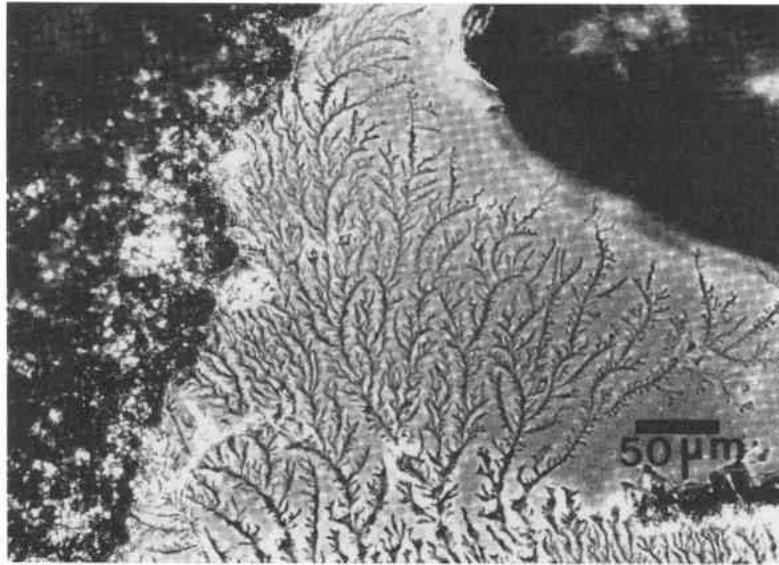


**Figure 7.** Thin dendritic halite crystals caused by surface layers (20  $\mu\text{g/ml}$ ) from *Haloarcula* SP8807. The bar represents 50  $\mu\text{m}$ .

The SDS-PAGE results were correlated with negatively stained preparations examined by transmission electron microscopy, which showed self-assembled S-layers (Figure 6). Despite the greater difficulty in obtaining good negatively stained S-layer from *Haloarcula* SP8807 strain, due to the high salt concentration and specific divalent cations required to maintain the integrity of the S-layer lattice (Koval & Murray, 1986; Kessel et al., 1988), a hint of periodicity and regions with honeycomb appearance of the morphological units was observed (Figure 6).

S-Layers of *Haloarcula* SP8807 (20  $\mu\text{g/ml}$ ) modified the crystal habit of halite, yielding dendritic crystals as well as cubic ones (Figure 7). The novel function of the cyanobacterial surface layer in fine-grain calcite formation proposed by Schultze-Lam et al. (1992) may be applicable to halite formation in the presence of halobacterial S-layer. This hypothesis, however, will require further study.

Our results show that halobacterial cells, and/or halobacterial S-layer protein, common in hypersaline ecosystems, are capable of inducing the formation of NaCl dendritic crystals. Supported by these results, we suggest the monitoring of organic carbon concentration and population density of halobacterial cells in crystallizer ponds of commercial salterns for the production of salt of high quality.

The dendritic crystals and their branches at micrometer level showed flat cubic microcrystals combined with amorphous crystals and halobacterial cells (Figure 4). The conservation and defects of the inner structure of these sodium chloride crystals will be studied in the future.

At low salt and magnesium concentration, spheroplasts prove to be extremely fragile (Jarrel & Sprott, 1984), and some lysis occurs. This is reflected by the many protein bands found in our SDS-PAGE. However, a 66-kDa light band was detected in the spheroplast samples (Figure 5). Jarrel and Sprott (1984) reported spherical bodies produced from logarithmic-phase cells, which were spheroplasts with cell wall still present but thinner than the wall of the original rod-shaped halobacterial cells.

**Table 2**  
Effect of dissolved and suspended materials in the formation of halite crystals

| Agent                    | Concentration<br>( $\mu\text{g}/\text{ml}$ ) | Shape                  | Relative<br>Abundance <sup>a</sup> | Frequency<br>(%) <sup>b</sup> |    |
|--------------------------|--|------------------------|------------------------------------|-------------------------------|----|
| Ferrocyanide             | 250  | Dendritic <sup>c</sup> | (+++)                              | 100                           |    |
| Glucose                  | 250  | Cubic                  | (+++)                              | 100                           |    |
| Glycerol                 | 250  | Cubic                  | (+++)                              | 100                           |    |
| Amino acids <sup>e</sup> | 200–2000                                     | Cubic                  | (+++)                              | 100                           |    |
| Casamino acids           | 200–600                                      | Cubic                  | (+++)                              | 100                           |    |
|                          |  | 1200                   | Dendritic <sup>d</sup>             | (++)                          | 15 |
|                          |  | Dendritic              | (+)                                | 55                            |    |
|                          | 2000   | Cubic                  | (++)                               | 30                            |    |
|                          |  | Dendritic <sup>d</sup> | (+++)                              | 10                            |    |
|                          |  | Dendritic              | (++)                               | 40                            |    |
|                          |  | Dendritic              | (+)                                | 40                            |    |
|                          |  | Cubic                  | (++)                               | 10                            |    |
| Silica gel               | 100–2000                                     | Cubic                  | (+++)                              | 100                           |    |
| Halobacteria cells       | 200 <sup>f</sup>                             | Dendritic <sup>d</sup> | (+++)                              | 50                            |    |
|                          |  | Cubic                  | (++)                               | 50                            |    |
| S-Layers                 | 20 <sup>g</sup>                              | Dendritic <sup>d</sup> | (+++)                              | 50                            |    |
|                          |  | Cubic                  | (++)                               | 50                            |    |

<sup>a</sup>(+++)  
Abundant, (++) common, (+) present.

<sup>b</sup>Frequency found in 60 experiments.

<sup>c</sup>Inside the cubic crystals (50  $\mu\text{m}$  average width of the branches).

<sup>d</sup>Between the cubic crystals (10  $\mu\text{m}$  average width of the branches).

<sup>e</sup>DL-Alanine, L(-)-proline, glycine, DL-serine, L-cysteine, DL-threonine, L(-)-tyrosine, L-histidine, L(+)-lysine, and L-glutamic acid.

<sup>f</sup>On basis of dry weight.

<sup>g</sup>On basis of Coomassie protein determination.

The effect of different chemical compounds on the induction of dendritic crystals of halite is shown in Table 2. As previously reported (Ploss, 1964; Shuman, 1965) and also shown in Table 2, ferrocyanide was capable of inducing the formation of dendritic crystals, but interestingly, the ferrocyanide salt at 250  $\mu\text{g}/\text{ml}$  caused dendritic growth of sodium chloride crystals entrapped within cubic crystals.

The poor formation of dendritic crystals by casein hydrolysate (1200–2000  $\mu\text{g}/\text{ml}$ ) suggests that some peptides could be responsible for this phenomenon. However, the amino acids do not induce the production of dendritic crystals (Table 2). The absence of dendritic crystal formation in the presence of silica gel demonstrated that this phenomenon is not the result of an inert particle effect.

In conclusion, the formation of a greater number of cubic crystals in the presence of halophilic archaeobacterial cells suggests that the cells serve as templates for halite formation.

The modification of the halite crystal habit, resulting in a dendritic shape, was attributed to the proteinaceous components of the S-layer of the halophilic archaeobacteria. Research on the types and concentrations of dissolved organic carbon compounds and halobacteria in natural solar salterns may be an important biotechnological tool in the operations of salterns.

## References

- Cohen, S., Oren, A., and Shilo, M. 1983. The divalent cation requirement of Dead Sea halobacteria. *Arch. Microbiol.* 136:184–190.
- Davis, J. S. 1978. Biological communities of a nutrient enriched salina. *Aquat. Bot.* 4:23–42.
- Grant, W. D., and Ross, H. N. M. 1986. The ecology and taxonomy of halobacteria. *FEMS Microbiol. Rev.* 39:9–15.
- Hecht, K., Wieland, F., and Jaenicke, R. 1986. The cell surface glycoprotein of *Halobacterium halobium*. *Biol. Chem.* 367:33–38.
- Jarrell, K. F., and Sprott, G. D. 1984. Formation and regeneration of *Halobacterium* spheroplast. *Curr. Microbiol.* 10:147–152.
- Javor, B. 1989. *Hypersaline environments*. New York: Springer-Verlag.
- Jones, A. G., Ewing, C. M., and Melvin, M. V. 1981. Biotechnology of solar saltfields. *Hydrobiology* 82:391–406.
- Kessel, M., Wildhaber, I., Cohen, S., and Baumeister, W. 1988. Three dimensional structure of the regular surface glycoprotein layer of *Halobacterium volcanii* from the Dead Sea. *EMBO J.* 7: 1549–1554.
- Koval, S. F., and Murray, R. G. E. 1986. The superficial protein array on bacteria. *Microbiol. Sci.* 3:357–361.
- Krumbein, W. E. 1985. Applied and economic aspects of sabkha systems—Genesis of salt, ore and hydrocarbon deposits and biotechnology. In *Hypersaline ecosystems*, eds. G. M. Friedman and W. E. Krumbein, pp. 426–436. New York: Springer-Verlag.
- Lechner, J., and Sumper, M. 1987. The primary structure of a procaryotic glycoprotein. *J. Biol. Chem.* 262:9724–9729.
- Lechner, J., and Wieland, F. 1989. Structure and biosynthesis of prokaryotic glycoproteins. *Annu. Rev. Biochem.* 58:173–194.
- Mescher, M. F., and Strominger, J. L. 1976. Purification and characterization of procaryotic glycoproteins from cell envelope of *Halobacterium salinarum*. *J. Biol. Chem.* 251:2005–2014.
- Mescher, M. F., Strominger, J. L., and Watson, S. W. 1974. Protein and carbohydrate composition of the cell envelope of *Halobacterium salinarum*. *J. Bacteriol.* 120:945–954.
- Messner, P., and Sleytr, U. B. 1991. Bacterial surface layer glycoproteins. *Glycobiology* 1:545–551.
- Messner, P., and Sleytr, U. B. 1992. Crystalline bacterial cell-surface layers. In *Advances in microbial physiology*, vol. 33, ed. A. H. Rose, pp. 213–275. New York: Academic Press.
- Norton, C., and Grant, W. D. 1988. Survival of halobacteria within fluid inclusions in salt crystals. *J. Gen. Microbiol.* 134:1365–1373.
- Ploss, R. S. 1964. Sodium chloride: Modification of crystal habit chemical agents. *Science* 144:143–144.
- Schneider, J., and Herrmann, A. G. 1980. Saltworks—Natural laboratories for microbiological and geochemical investigations during the evaporation of seawater. *5th Symp. Salt 2*, eds. A. H. Coogan and L. Hauder, pp. 371–381. Cleveland, Ohio: North Ohio Geological Society.
- Schultze-Lam, S., Harauz, G., and Beveridge, T. J. 1992. Participation of a cyanobacterial S layer in fine-grain mineral formation. *J. Bacteriol.* 174:7971–7981.
- Shuman, A. C. 1965. Gross imperfections and habit modification in salt crystals. *2nd Symp. Salt 12*, ed. J. L. Rau, pp. 246–253. Cleveland, Ohio: North Ohio Geological Society.
- Sleytr, U. B., Messner, P., and Pum, D. 1988. Analysis of crystalline bacterial surface layers by freeze-etching, metal shadowing, negative staining and ultrathin sectioning. In *Methods in microbiology*, vol. 20, ed. F. Mayer, pp. 29–60. New York: Academic Press.
- Sumper, M. 1987. Halobacterial glycoprotein biosynthesis. *Biochim. Biophys. Acta* 906:69–79.
- Sumper, M., Berg, E., Mengele, R., and Strobel, I. 1990. Primary structure of glycosylation of the S-layer protein of *Haloferax volcanii*. *J. Bacteriol.* 172:7111–7118.
- Torreblanca, M., Rodríguez-Valera, F., Juez, G., Ventosa, A., Kamekura, M., and Kates, M. 1986. Classification of nonalkaliphilic halobacteria based on numerical taxonomy and polar lipid composition, and description of *Haloarcula* gen. nov. *System. Appl. Microbiol.* 8:89–99.
- Van-Seuningen, I., and Davril, M. 1992. A rapid periodic acid-Schiff staining procedure for the detection of glycoproteins using the PhastSystem. *Electrophoresis* 13:97–99.